Theoretical Investigation on the Nuclear Quadrupole Interaction of CH_3Cl, CH_2Cl_2 and $CHCl_3$ *

Gerald Frantz **, Hagen Dufner, and P. C. Schmidt

Institut für Physikalische Chemie, Technische Hochschule Darmstadt, D-64287 Darmstadt, Germany

Z. Naturforsch. **49a**, 116–124 (1994); received November 11, 1993

The nuclear quadrupole interaction of ^{35}Cl in CH_3Cl, CH_2Cl_2 and $CHCl_3$ has been studied theoretically by the Hartree-Fock-Roothaan procedure. The influence of the crystal field on the nuclear quadrupole coupling constant is incorporated by the cluster approach and by using point charges that are consistent with the external potential.

Introduction

The nuclear quadrupole interaction in Cl-substituted methanes $CH_{4-n}Cl_n$, $n=1$ to 3, has been investigated extensively by experimental [1–7] and theoretical [8–10] methods. The nuclear quadrupole coupling constant ν (NQCC) is expressed as

$$\nu = q(eQ/h), \tag{1}$$

where q is the largest component of the electric field gradient (EFG) tensor in the principal axis system at a given nucleus.

In the gas phase the NQCC's for $CH_{4-n}Cl_n$ are gained from microwave [1, 2] and molecular beam measurements [3], whereas in the solid state the values of ν are deduced from NQR and NMR studies [4, 6, 7]. Theoretically, q is calculated for the isolated molecules CH_3Cl [8–10] and $CHCl_3$ [9] in the gas phase by ab initio self consistent field (SCF) calculations using Gaussian basis sets [11].

The gas phase value of $\nu(^{35}Cl)$ increases from CH_3Cl to $CHCl_3$ by about 10%. This trend can be understood simply by considering the electronegativity: with increasing number of Cl atoms each Cl becomes less negatively charged, and therefore the charge around the Cl nucleus becomes more asymmetric. Considering the occupation numbers, the occupation of the $3p_z$ orbital along the Cl–C bond axis is decreasing with increasing number of Cl atoms, whereas the occupation of the $3p_x$ and $3p_y$ orbitals are almost constant. Comparing the experimental EFG at the chlorine site with theoretical results from ab initio SCF calculations, differences of about 1.2–6% for CH_3Cl [8–10] and 10% for $CHCl_3$ [9] are found.

In the solid state the compounds crystallize in different structures [12–14] which are displayed in Figure 1. Considering the chlorine nuclei, there is only one crystallographic position in the unit cell of CH_3Cl and CH_2Cl_2, and one resonance line for the chlorine nuclei is found for these compounds [4, 6, 7]. In $CHCl_3$, however, there are two non equivalent chlorine positions labeled a and b in Fig. 1, and two resonance lines for ^{35}Cl are detected [6, 7]. From the line width analysis and the intensity of the lines it follows that the resonance line for the position Cl_a occours at a lower frequency than for the position Cl_b [15].

Comparing the gas phase and solid state data one obtains that the $\nu(^{35}Cl)$ in the solid state is between 6% and 9% smaller than in the gas phase. This influence of the surrounding molecules, here called the solid state effect, leads to a decrease of the EFG at the chlorine nucleus. This solid state effect is explained qualitatively by the change of the Cl–C distance on going from the gas phase [16–18] to the solid state, and furthermore by intermolecular Cl–H bonds in the crystal [12, 19].

In the present paper we study the nuclear quadrupole interaction in these compounds by quantum mechanical calculations at the ab initio SCF level. We wanted to find out whether the results of our calculation can verify quantitatively the trends in the ν's reported above, and furthermore whether the origin of the trends can be explained in a simple quantum mechanical picture.

* Presented at the XIIth International Symposium on Nuclear Quadrupole Resonance, Zürich, Switzerland, July 19–23, 1993.

** Part of Dr.-Ing. thesis of Gerald Frantz, Technische Hochschule Darmstadt, D17.

Reprint requests to Prof. Dr. P. C. Schmidt, Physikalische Chemie I, TH Darmstadt, Petersenstraße 20, D-64287 Darmstadt, Germany.

0932-0784 / 94 / 0100-0116 $ 01.30/0. – Please order a reprint rather than making your own copy.

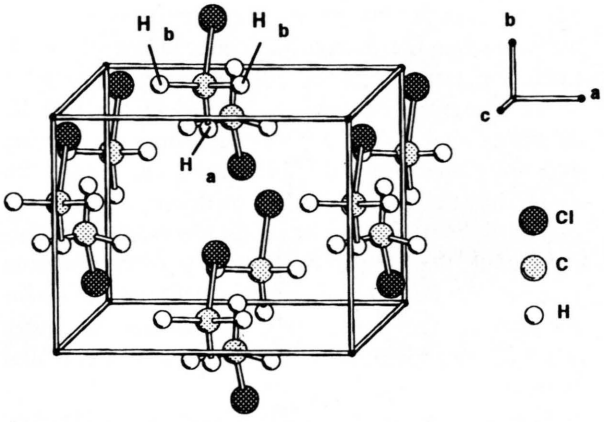

CH_3Cl

orthorhombic
C_{2v}^{12} – Cmc2_1 (no. 36)
$Z=4$
$a=649.5$ pm
$b=513.9$ pm
$c=752.3$ pm

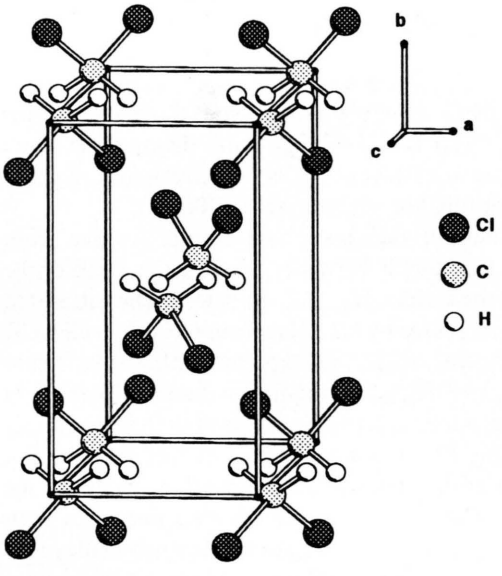

CH_2Cl_2

orthorhombic
D_{2h}^{14} – Pbcn (no. 60)
$Z=4$
$a=424.9$ pm
$b=813.8$ pm
$c=949.2$ pm

Fig. 1. Crystal structure of CH_3Cl [12], CH_2Cl_2 [13] and $CHCl_3$ [14].

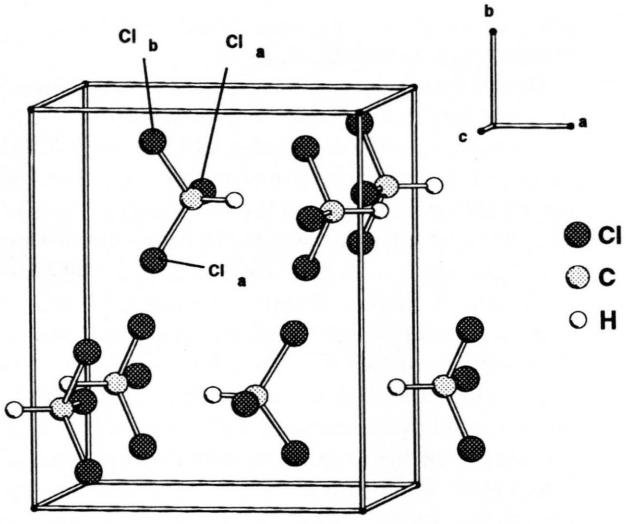

$CHCl_3$

orthorhombic
D_{2h}^{16} – Pnma (no. 62)
$Z=4$
$a=748.5$ pm
$b=949.7$ pm
$c=584.1$ pm

Method

The nuclear quadrupole interaction is characterized by the coupling constant ν, Eq. (1), and the asymmetry parameter η,

$$\eta = \frac{q_{XX} - q_{YY}}{q_{ZZ}},$$

where (X, Y, Z) is the principal axis system and $q = q_{ZZ} > q_{YY} > q_{XX}$.

Computationally the EFG tensor is initially obtained in terms of the x, y, and z coordinates of the input geometry. For example, the component q_{zz} of the total EFG is the sum of the contribution of the nuclei

$$q_{zz}^{(n)} = e \sum Z_i \frac{3z_i^2 - r_i^2}{r_i^5}$$

and the electronic part

$$q_{zz}^{(el)} = -e \int \varrho(r) \frac{3z^2 - r^2}{r^5} \, d\tau \, .$$

Here Z_i are the atomic numbers and $\varrho(r)$ is the electron density obtained from the ab initio SCF calculation. Diagonalization of the tensor q_{ij}, $i,j = x,y,z$,

gives the components q_{XX}, q_{YY}, and q_{ZZ} and the angles between (x, y, z) and (X, Y, Z).

The SCF calculations have been performed using the programs HONDO [20] and GAUSSIAN 90 [21]. It was pointed out in earlier theoretical investigations on the EFG in chlorine compounds [8–10] that one should use extended basis sets including d functions at Cl and C and p functions at H. Additionally we have found that one should have more than one p function at the chlorine site to describe the valence electrons and one should include also one d basis function centered at the hydrogen site. There are several basis sets of this type published in the literature [22]. Using a nuclear quadrupole moment $Q(^{35}Cl) = -0.082$ barn [23] we get the best agreement with the experimental values of the EFG with the following basis set: a (12s, 9p, 1d)/[6s, 4p, 1d] basis [24, 25] for Cl, a (10s, 5p, 1d)/[3s, 2p, 1d] basis [26] for C, and a (4s, 1p, 1d)/[2s, 1p, 1d] basis [27] for H. We have used these basis functions for all calculations of the present paper.

The influence of the surrounding molecules on the electronic states can be investigated by different methods. First, one can perform a band structure calculation using either the Hartree-Fock approximation [28] or the density functional method [29]. Second, within the molecular orbital approach one can calculate the electronic properties for a cluster of several molecules taking the solid state geometry for the atomic positions. Additionally, external point charges can simulate the crystal field of the remaining lattice [30, 31].

As we want to compare the gas phase and the solid state data it is useful to use the same method for both phases. Therefore we have chosen the cluster method for the investigation of the crystal field effect. To study various contributions to the total solid state effect we have performed several model calculations, called model 1 to 4 below. First we have calculated the EFG for a monomer using, however, the geometry found for the solid state instead of the gas phase geometry (model 1). Figure 2a shows the slightly different internal coordinates of CH_3Cl for the solid state [12] and the gas phase [32]. Next we have described the influence of the monomer's surrounding by point charges (model 2). Third we have performed the molecular SCF calculation for a cluster of three to four molecules (model 3); see Figure 2b for the case of CH_3Cl. Finally we have simulated the influence of the rest of the lattice for this cluster again by point charges (model 4). The positions of the point charges are chosen at the atomic positions of the crystal structure. The values of the charges are chosen in two ways. First we have taken the charges q_{Mul} deduced from the Mulliken population analysis [33]. Second we have used potential-derived charges q_{pdc} [34], which describe the multiple moments of the molecules quite well [34]. The q_{pdc} are gained from the following least squares fit. From the calculated SCF electron density distribution $\varrho(\boldsymbol{r})$ of the molecule or cluster the electrostatic potential outside the van der Waals volume of the molecule is calculated on a grid of points. Then those values for the point charges at the atomic positions of the cluster are determined which give the best fit to this potential function.

Furthermore we have deduced $\varrho(\boldsymbol{r})$ and q_{pdc} in a self consistent procedure. We have used the fitted point charges to obtain the external potential of an infinite lattice. This external potential is included in the molecular SCF calculation to recalculate $\varrho(\boldsymbol{r})$. This procedure is performed until the difference of the charges between the previous run and the actual run has been reached a certain threshold.

Results and Discussion

The EFG at the chlorine site is calculated for CH_3Cl, CH_2Cl_2 and $CHCl_3$ using the basis set given in the previous section. The experimental and theoretical results are summarized in Table 1.

Considering the gas phase results we see from Table 1 that the SCF results describe the trend of the EFG in the series $CH_{4-n}Cl_n$ quite well. The calculated NQCC increases by 1.2 MHz from CH_3Cl to CH_2Cl_2 which agrees with the experimental result. From CH_2Cl_2 to $CHCl_3$ the theory predicts an increase of 5.0 MHz, which is 1.1 MHz larger than the experimental finding. The reason for the increase of the EFG can be seen from the orbital population analysis, see Table 1. The ionicity of the chlorine decreases with increasing n, and according to the Townes-Dailey theory [35] the EFG also increases. However there is no linear dependence of the EFG on the orbital population, or on the occupation of the $3p_z$ orbital n_{pz}, see Figure 3. This can be explained in the following manner. At the chlorine site the valence electron states are described by two s, two p and one d function centered at the chlorine atom. The major contribution to the EFG comes from the two p basis functions given in Table 2. From Table 2 we can see that the function f_1

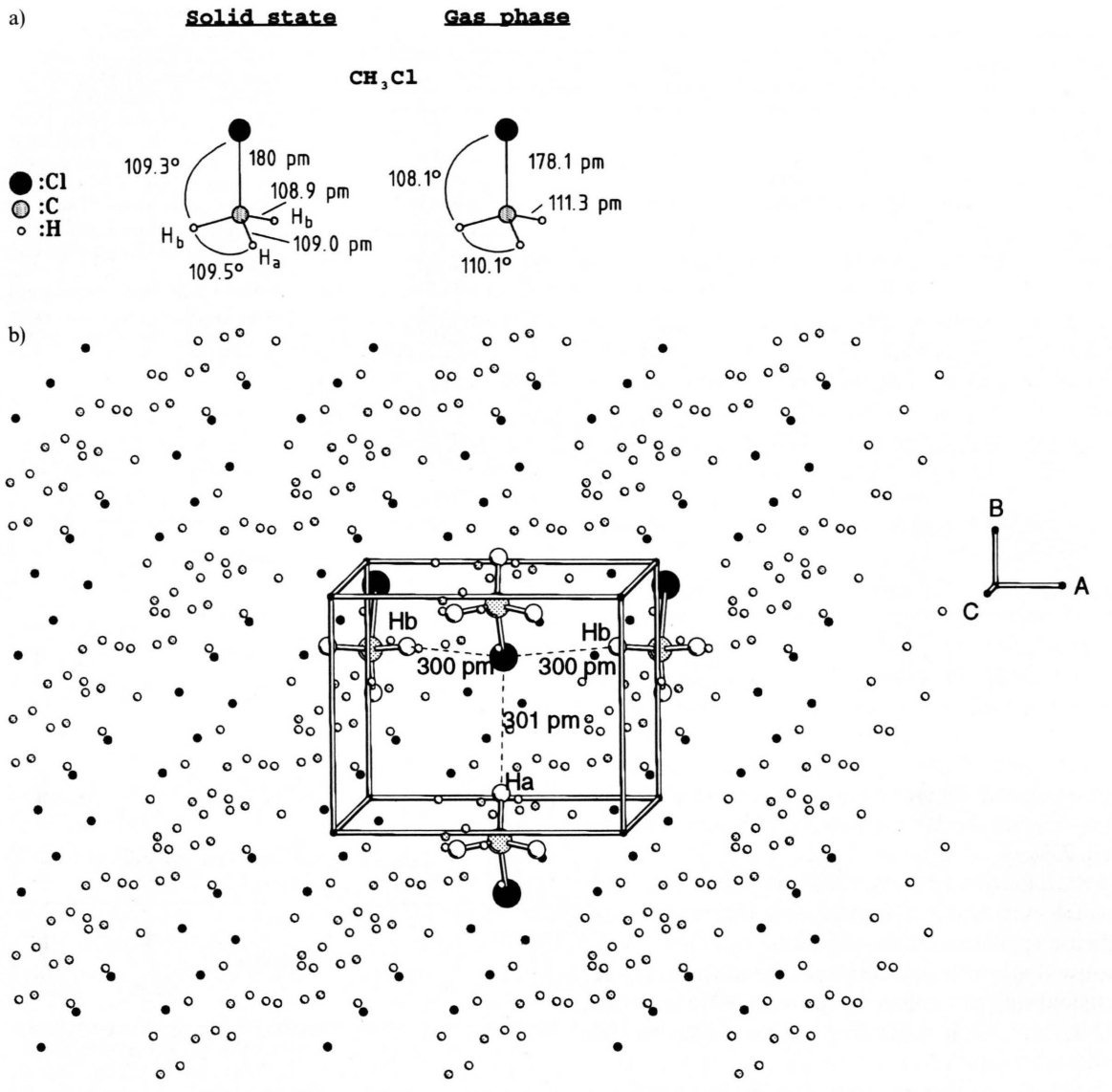

Fig. 2. a) Gas phase [32] and solid state [12] geometry of $CHCl_3$. b) Cluster and point charges for the solid state calculation of CH_3Cl.

is more localized than the function f_2, and therefore the radial integral of the EFG I_1,

$$I_1 = \int \frac{f_1^2}{r^3} r^2 \, dr ,$$

is larger than the corresponding integral I_2. It follows that the calculated EFG depends on two parameters, on the overall $3p_z$ occupation

$$n_{p_z} = n_{p_{z1}} + n_{p_{z2}} ,$$

and additionally on the ratio $r_{1,2} = \frac{n_{p_{z1}}}{n_{p_{z2}}}$ of the partial contributions of the functions f_1 and f_2. The change of $r_{1,2}$ describes the change of the character of the 3p orbital as a function of ionicity of chlorine. For example the normalized 3p state for the Cl^- is more diffuse than for Cl^0, see Figure 4. In Fig. 3 the calculated EFG is also plotted as function of the partial occupation numbers $n_{p_{z1}}$ (**1**) and $n_{p_{z2}}$ (**2**) of the function f_1 and f_2 for the chlorine 3p state. We see that the EFG

Compound	Experimental results			Theoretical results			
	EFG [a.u.]	$\nu(^{35}Cl)$ [MHz]	η	EFG [a.u.]	$\nu(^{35}Cl)$ [MHz]	q_{Mul}	η
gas phase							
CH_3Cl	−3.877	74.69 [3]	0.000	−3.869	73.76	−0.199	0.000
CH_2Cl_2	−3.971	76.50 [17]	0.000	−3.930	75.45	−0.160	0.035
$CHCl_3$	−4.173	80.39 [1]	0.000	−4.169	80.51	−0.111	0.002
solid state							
CH_3Cl	−3.579	68.75 [19]	0.000	-3.614^{I}	69.615^{I}	-0.263^{I}	0.004
				-3.603^{II}	69.403^{II}	-0.251^{II}	0.004
CH_2Cl_2	−3.762	72.49 [15]	0.068 [7]	-3.781^{I}	72.832^{I}	-0.192^{I}	0.046
				-3.802^{II}	73.237^{II}	-0.183^{II}	0.055
$CHCl_3$	−4.003	77.02 [15]	0.040 [7]	$-4.055^{a,I}$	$78.110^{a,I}$	$-0.118^{a,I}$	0.016
				$-4.064^{a,II}$	$78.283^{a,II}$	$-0.115^{a,II}$	0.019
			0.057 [7]	$-4.091^{b,I}$	$78.804^{b,I}$	$-0.119^{b,I}$	0.007
				$-4.077^{b,II}$	$78.534^{b,II}$	$-0.123^{b,II}$	0.002

Table 1. Theoretical and experimental values of the NQCC $\nu(^{35}Cl)$ and electric field gradient (EFG) at the chlorine site in $CH_{4-n}Cl_n$. The experimental solid state results are the extrapolated values for 0 K. A quadrupole moment $Q(^{35}Cl) = -0.082$ barn [23] is used. The two theoretical values I and II belong to model 2 and model 4, respectively, of Table 2, see below. For the compound $CHCl_3$ the values for both crystallographic sites a and b (Figure 1) are given.

Table 2. The two 3p basis functions f_1 and f_2 of the chlorine basis set [24].

p basis function	Exponent	Coefficient
f_1	0.950083	1.00000
f_2	0.358271	0.55450
	0.124986	0.31609

depends almost linearly on the occupation of f_1 because f_1 gives the largest radial contribution to the EFG [36].

Next, differences between the gas phase data and the solid state data will be discussed. The solid state ν is always smaller than the gas phase ν. This trend is also found in our theoretical study. Quantitatively, the calculated shift of ν differs by up to 1.5 MHz from the experimental result depending on the chosen model for the solid state effect.

The result are shown in detail in Table 3 and Figure 5. In Table 3 the occupation numbers and the calculated EFG for the different model calculations described above are given. The first line shows again the results for the monomer using the gas phase geometry.

The second line (model 1) gives the results for the monomer, however, using the atomic positions found for the solid state. We see that the change of the geometry has a minor effect on the EFG for CH_3Cl, whereas for CH_2Cl_2 and $CHCl_3$ the change in the geometry causes a distinct decrease of ν. Furthermore the differences of ν for the positions *a* and *b* for $CHCl_3$ are larger than the experimental findings [15, 37].

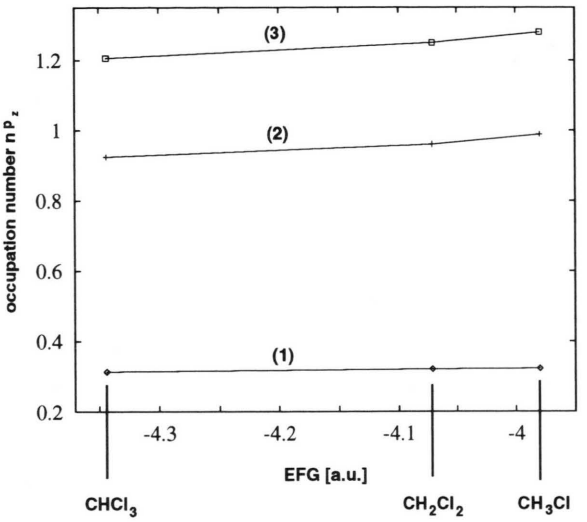

Fig. 3. Correlation between the calculated EFG and the occupation number n_{p_z} (**3**) for the chlorine 3p state. Additionally the correlation between the EFG and the partial occupation number $n_{p_{z1}}$ and $n_{p_{z2}}$ belonging to the function of f_1 (**1**) and f_2 (**2**) of Table 2 are shown.

The structure data are from measurements at 77 K. At this temperature the experimental values are $\nu(^{35}Cl_a) = 76.51$ MHz and $\nu(^{35}Cl_b) = 76.62$ MHz [15, 37].

In the third line of Table 3 (model 2) we have included the external field of the surrounding molecules within the point charge model using the potential derived charges as external charges. The field of the external charges distinctly influences the EFG and results in a decrease of the EFG in accordance with the experimental finding. We see that the chlorine

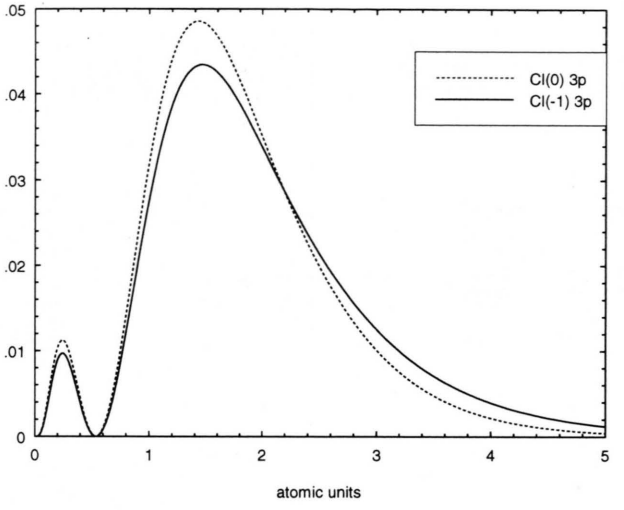

Fig. 4. Radial density $P^2_{3p}(r)$ of a normalized 3p function for the free chlorine atom and anion calculated by the local density approximation.

atom becomes slightly more negatively charged in the solid state and therefore the EFG is decreasing. The reason for the small charge transfer to the chlorine can be seen from Fig. 6, in which we have plotted the external potential for an electron along the bonding axis H–C and C–Cl. The potential is negative in the region of the chlorine and positive in the region of the carbon and hydrogen and results in a shift of electronic charge to the chlorine.

Returning to the model calculations given in Fig. 5 and Table 3, we see in the fourth line the results for a cluster calculation (model 3). The cluster used is displayed in Fig. 2b for the case of CH_3Cl. Comparing the monomer with the cluster result we see that the trend is the same as that found on the inclusion of the point charges. However, the change of the EFG and the Mulliken charge at the chlorine site q_{Mul} is smaller than the change found on inclusion of the point charges.

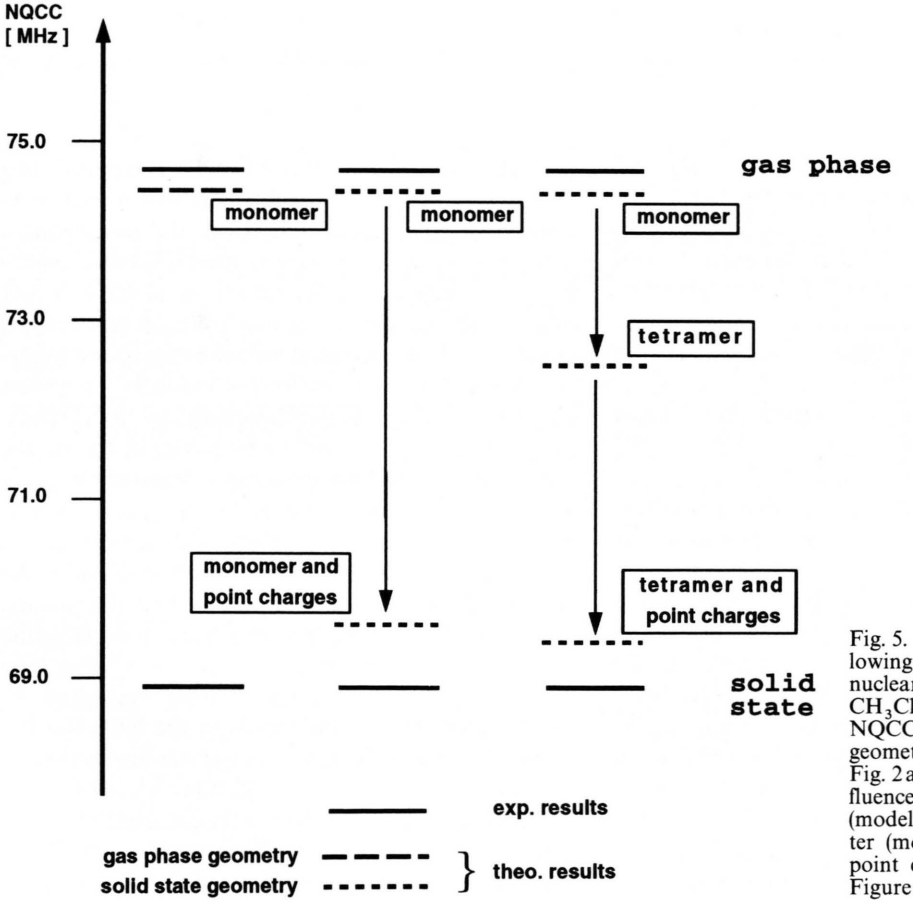

Fig. 5. Scheme to display the following solid state effects on the nuclear quadrupole interaction in CH_3Cl. (1) Change of the calculated NQCC going from the gas phase geometry to the solid geometry (see Fig. 2a, model 1 in the text); (2) Influence of the external point charges (model 2); (3) Influence of the cluster (model 3); (4) Influence of the point charges on the cluster, (see Figure 2b, model 4).

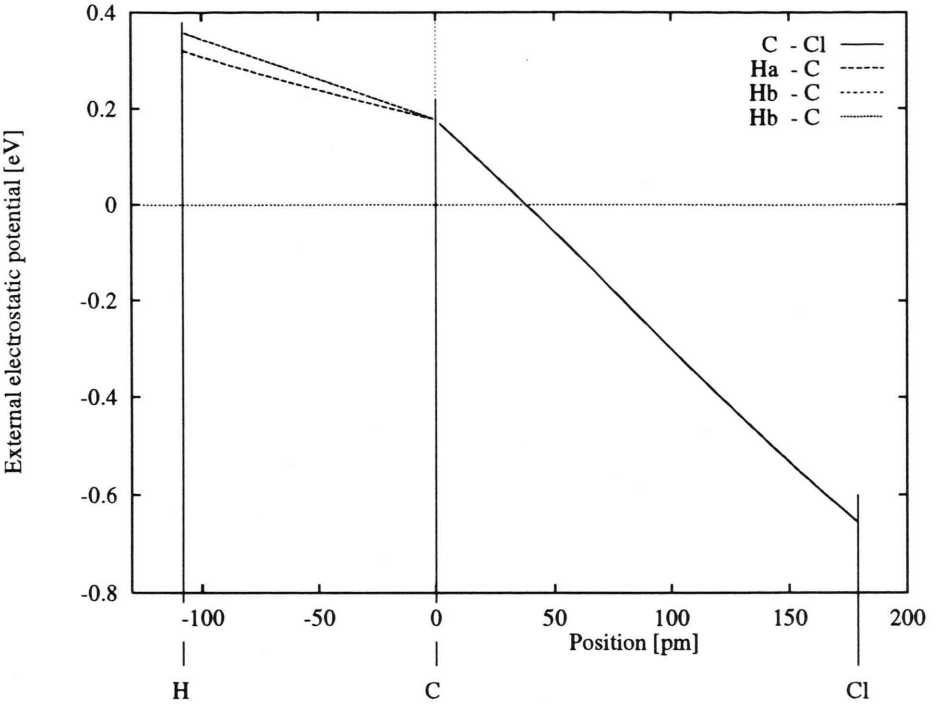

Fig. 6. External electrostatic potential for an electron along the H–C and C–Cl direction calculated in CH_3Cl from the potential derived charges.

Table 3. Theoretical results of the NQCC $\nu(^{35}Cl)$, the Mulliken charges q_{Mul}, the potential derived charges q_{pdc} and the asymmetry parameter η at the chlorine in Cl substituted methanes $CH_{4-n}Cl_n$, $n=1$ to 3. The values are given for the different models discussed in the text, see also Figure 5. In the case of $CHCl_3$ the values are given for both crystallographic sites, see Figure 1.

Compound	Model	$\nu(^{35}Cl)$ [MHz]	q_{Mul}	q_{pdc}	η
CH_3Cl	gas phase	74.527	−0.199	−0.206	0.0000
	model 1	74.547	−0.212	−0.218	0.0009
	model 2	69.615	−0.263	−0.273	0.0037
	model 3	72.447	−0.221	−0.154	0.0014
	model 4	69.403	−0.251	−0.185	0.0037
CH_2Cl_2	gas phase	75.702	−0.160	−0.154	0.0351
	model 1	74.932	−0.165	−0.164	0.0464
	model 2	72.832	−0.192	−0.194	0.0502
	model 3	74.431	−0.168	−0.176	0.0554
	model 4	73.237	−0.183	−0.184	0.0655
$CHCl_3Cl_a$	gas phase	80.306	−0.111	−0.076	0.0020
	model 1	78.842	−0.109	−0.074	0.0050
	model 2	78.110	−0.118	−0.084	0.0164
	model 3	78.765	−0.106	−0.090	0.0137
	model 4	78.283	−0.115	−0.110	0.0192
$CHCl_3Cl_b$	model 1	79.093	−0.111	−0.074	0.0028
	model 2	78.804	−0.119	−0.079	0.0071
	model 3	78.187	−0.125	−0.069	0.0026
	model 4	78.534	−0.123	−0.069	0.0024

In the last line of Table 3 (model 4) we have displayed the results using the cluster model and additionally for the rest of the lattice the point charge model. These calculations are extremely time consuming and one sees that the results of model 4 do not differ significantly from the much simpler calculations of model 2. The agreement between theory and experiment is almost the same for both models. Therefore, studying $\nu(^{35}Cl)$ in molecular crystal by the Hartree-Fock procedure it seems to be sufficient to use the point charge model for the incorporation of the intermolecular effects. This should be different if correlation effects are included in the calculations.

We also used the Mulliken charges to simulate the external point charges in a self consistent manner. These results differ significantly from those with the potential derived point charges given in Table 3 by about 100–700 kHz. These results are given in Table 4. We see that the trends in the EFG are described much more satisfactority by the potential derived charges than by the Mulliken charges.

Finally we have investigated the calculated EFG as a function of the position of the hydrogen nuclei. The results are presented in Figure 7. In Fig. 7a the total

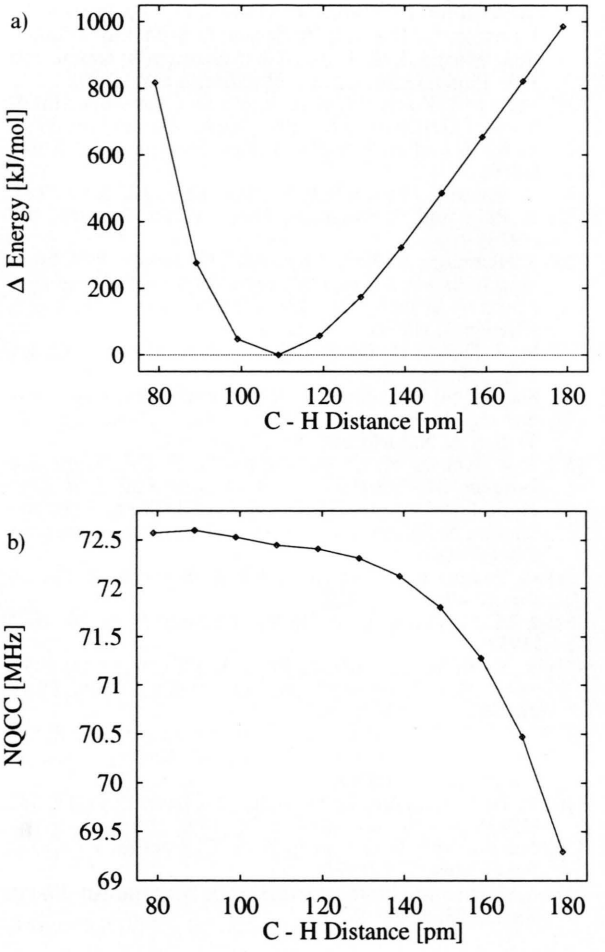

Fig. 7. Total energy and the NQCC as a function of the H–Cl distance for a cluster of four CH_3Cl molecules.

energy of a CH_3Cl cluster (model 3) is plotted as a function of the H–Cl distance. The minimum of the total energy is found at about 110 pm, which is equal to the value reported by Burbank [12] and which is also used in our calculations reported above. Figure 7b shows the EFG at the Cl nuclei as a function of the H–Cl distance. The change of the H–Cl distance by ±10 pm changes the calculated EFG by about 100 kHz. Therefore the Hartree-Fock model predicts only a small effect of the H–Cl bonding on the EFG. However, to study the hydrogen-bonding effect in detail, one has to incorporate correlation effects which could not be included here.

Table 4. Theoretical results of the NQCC $\nu(^{35}Cl)$ using the Mulliken charges q_{Mul} instead of the potential derived charges (Table 3) to simulate the solid state. The values are given for the different models discussed in the text. In the case of $CHCl_3$ the values are given for both crystallographic sites, see Figure 1.

Compound	Model	$\nu(^{35}Cl)$ [MHz]	q_{Mul}	η
CH_3Cl	model 2	69.018	−0.268	0.0039
	model 4	68.691	−0.257	0.0044
CH_2Cl_2	model 2	72.582	−0.195	0.0503
	model 4	73.610	−0.185	0.0665
$CHCl_3Cl_a$	model 2	78.100	−0.119	0.0189
	model 4	78.340	−0.115	0.0198
$CHCl_3Cl_b$	model 2	78.707	−0.121	0.0087
	model 4	78.361	−0.126	0.0024

Conclusions

In the present work it is shown that the Hartree-Fock-Roothaan procedure describes the nuclear quadrupole coupling constant of ^{35}Cl in the compounds $CH_{4-n}Cl_n$ quantitatively if one uses large Gaussian basis sets. The intermolecular field of potential derived point charges obtained by a self consistent procedure describes the crystal field effect on the EFG quite well.

In the solid state the chlorine is slightly more negatively charged than in the gas phase. Due to this small charge transfer, a decrease of the NQCC in the solid state compared to the gas phase is observed. This charge transfer can be explained by a small attractive crystal field for the electrons at the chlorine.

Acknowledgements

We gratefully thank the Deutsche Forschungsgemeinschaft and the Fonds der Chemischen Industrie for support of this work. We also thank Dipl.-Phys. W. Reichenbächer from the Rechenzentrum der THD for help.

[1] P. N. Wolfe, J. Chem. Phys. **25,** 976 (1965).
[2] W. Gordy, J. W. Simmons, and A. G. Smith, Phys. Rev. **72,** 344 (1947); Phys. Rev. **74,** 243 (1948).
[3] S. G. Kukolich, and A. C. Nelson, J. Amer. Chem. Soc. **95,** 680 (1973).
[4] J. L. Ragle and K. L. Sherk, J. Chem. Phys. **50,** 3553 (1969).
[5] P. C. M. van Zijl and A. A. Bothner-By, J. Magn. Reson. **79,** 439 (1988).
[6] R. Livingston, Phys. Rev. **82,** 1434 (1951).
[7] G. Litzistorf, S. Sengupta, and E. A. Lucken, J. Magn. Resonance **42,** 307 (1980).
[8] M.-C. Montabouel, M. Suard, and L. Guibe, Mol. Phys. **40,** 1503 (1980).
[9] J. Kowalewski and K. M. Larsson, Chem. Phys. Lett. **109,** 404 (1984).
[10] G. L. Bendazzoli, D. G. Lister, and P. Palmeri, J. Chem. Soc., Faraday Trans. **69,** 791 (1973).
[11] E. Clementi and D. R. Davis, J. Chem. Phys. **45,** 2593 (1966); J. Computational Phys. **2,** 223 (1967).
[12] R. D. Burbank, J. Amer. Chem. Soc. **75,** 1211 (1953).
[13] T. Kawaguchi, K. Tanaka, T. Takeuchi, and T. Watanabe, Bull. Chem. Soc. Japan **46,** 62 (1973).
[14] R. Fourme and M. Renaud, C. R. Acad. Sci. Paris Ser. B **263,** 69 (1969).
[15] H. S. Gutowsky and D. W. McCall, J. Chem. Phys. **32,** 548 (1960).
[16] S. L. Miller, L. C. Aamodt, G. Dousmanis, and C. H. Townes, J. Chem. Phys. **20,** 1112 (1952).
[17] R. J. Myers and W. D. Gwinn, J. Chem. Phys. **20,** 1420 (1952).
[18] S. N. Ghosh, R. Trambarulo, and W. Gordy, J. Chem. Phys. **20,** 605 (1952).
[19] G. A. Monti, C. A. Martin, D. Rupp, and E. A. C. Lucken, J. Phys. C: Solid State Phys. **21,** 3023 (1988).
[20] HONDO-8, M. Dupuis, J. D. Watts, H. O. Villar, and G. J. B. Hurst, Program no. 544, Quantum Chemistry Program Exchange, India University, Bloomington, India.
[21] Gaussian 90, M. J. Frisch, M. Head-Gordon, G. W. Trucks, J. B. Foresman, H. B. Schlegel, K. Raghavachari, M. A. Robb, J. S. Binkly, C. Gonnzalez, D. J. Defrees, D. J. Fox, R. A. Whiteside, R. Seeger, C. F. Melius, J. Baker, R. L. Martin, L. R. Kahn, J. J. P. Stewart, S. Topioi, and J. A. Pople, Gaussian Inc. Pittsburgh PA, (1990).
[22] See e.g. R. Poirier, R. Kari, and J. G. Csizmadia, Handbook of Gaussian basis sets, Elsevier Amsterdam, 1985.
[23] V. Kellö and A. J. Sadlej, Chem. Phys. Lett. **174,** 641 (1990).
[24] A. Veillard, Theoret. Chim. Acta (Berl.) **12,** 405 (1968).
[25] B. Roos and P. Siegbahn, Theor. Chim. Acta **17,** 199 (1970).
[26] S. Huzinaga, J. Chem. Phys. **42,** 1293 (1965); T. H. Dunning Jr. and P. J. Hay in Modern Theoretical Chemistry, edited by Schaefer III, H. F. Plenum, New York, Vol. 3, Chapter **1,** (1977).
[27] W. J. Hehre, R. Ditchfield, and J. A. Pople, J. Chem. Phys. **56,** 2257 (1972).
[28] See e.g. M. H. Palmer, Z. Naturforsch. **49a,** 146 (1994).
[29] See e.g. P. Blaha, K. Schwarz, G. Vielsack, and W. Weber, Z. Naturforsch. **49a,** 129 (1994).
[30] P. C. Kelires, K. C. Mishra, and T. P. Das, Hyperfine Interact. **34,** 289 (1987); P. C. Kelires and T. P. Das, Hyperfine Interact. **34,** 285 (1987); J. Stein, S. B. Sulaiman, N. Sahoo, and T. P. Das, Hyperfine Interact. **60,** 849 (1991).
[31] G. Frantz, R. Leiberich, and P. C. Schmidt, Z. Naturforsch. **47a,** 182 (1992).
[32] J. M. Mays and B. P. Dailey, J. Chem. Phys. **20,** 1695 (1952).
[33] R. S. Mulliken, J. Chem. Phys. **3,** 573 (1935); **23,** 1833, 1841, 2338, 2343 (1955); **36,** 3428 (1962); J. Chim. Phys. **46,** 497, 675 (1949).
[34] L. E. Chirlian and M. M. Francl, J. Comp. Chem. **8,** 894 (1987); C.M. Brennemann and K. B. Wiberg, J. Comp. Chem. **11,** 361 (1990).
[35] C. H. Townes and B. P. Dailey, J. Chem. Phys. **17,** 782 (1949).
[36] See also the discussion in E. A. C. Lucken, Z. Naturforsch. **49a,** 133 (1994).
[37] V. Harihara Subramanian and P. T. Narasimhan, J. Mol. Struct. **83,** 117 (1982).